Contents lists available at ScienceDirect

Separation and Purification Technology

journal homepage: www.elsevier.com

Photocatalytic degradation of thiobencarb by a visible light-driven MoS_2 photocatalyst

Shiyun Huang[a], Chiingchang Chen[b], Hweiyan Tsai[a], Janah Shaya[c], Chungshin Lu[d,*]

[a] School of Medical Applied Chemistry, Chung Shan Medical University, Taichung 402, Taiwan, ROC
[b] Department of Science Application and Dissemination, National Taichung University of Education, Taichung 403, Taiwan, ROC
[c] Institut de Physique et Chimie des Matériaux (IPCMS), UMR 7504, CNRS-Université de Strasbourg, 23 Rue du Loess, 67034 Strasbourg Cedex 2, France
[d] Department of General Education, National Taichung University of Science and Technology, Taichung 403, Taiwan, ROC

ARTICLE INFO

Keywords:
MoS_2
Photocatalysis
Visible light
Thiobencarb
Pathway
Water treatment

ABSTRACT

In this study, molybdenum disulfide (MoS_2) microsphere was prepared and employed as a visible-light catalyst for the photocatalytic degradation of thiobencarb (TBC), a carbamate pesticide. The as-prepared MoS_2 photocatalyst was characterized by X-ray diffraction (XRD), scanning electron microscopy (SEM), and X-ray photoelectron spectroscopy (XPS). TBC elimination using MoS_2 proved to be efficient and practical in both deionized and environmental water samples. This photocatalytic method presented a set of advantages over other TBC removal processes such as using visible light source without the need of costly additives (e.g.·H_2O_2). Optimization studies of this process showed that the degradation efficiency could reach 95% in 12 h at a pH range of 6–9. Further, the effect of anions (Cl^- and NO_3^-) was minor on the photocatalytic activity of MoS_2. Experiments using radical scavengers indicated that hydroxyl radicals and holes are the prevailing reactive species involved in this process. Three possible photodegradation pathways were proposed based on the major intermediates as verified by gas chromatography/mass spectrometry technique. The practicality of this MoS_2 photocatalyst was validated by its use in the removal of TBC from real water samples and by its stability and reusability in three successive runs, evidencing its prospective applications in the treatment of environmental water and contaminated wastewater samples.

1. Introduction

Carbamates are used as one of the main classes of the widely consumed pesticides in the world [1]. Indeed, this family is well known for the diversity of its biological activity so that it is utilized as insecticides, fungicides, nematocides, miticides, and molluscicides [2]. Carbamates are recognized with their toxicological effects to environment and specifically to human beings by their neurological effects as acetylcholinesterase inhibitors [3]. The United States Environmental Protection Agency (EPA) included carbamates on the priority list of pollutants [4]. The major problem with usage of carbamates is their persistence in the environment that might last for many years for certain compounds. Owing to their high solubility in water, their residues can circulate in aqueous mediums by leaching and runoff from soil into ground and surface water [5]. Furthermore, their broad applications in agriculture result in raising their residues in environmental matrices.

In particular, thiobencarb (TBC, S-4-chlorobenzyl diethylthiocarbamate) represents a carbamate pesticide frequently used in rice fields. The chemical structure of TBC is displayed in Fig. 1. The worldwide rate of TBC consumption is around 18,000 tons per year (40 countries) [6]. TBC has been detected in river waters constituting a threat to the aquatic ecosystem due to its resistance to degradation by hydrolysis and its moderate toxicity in acute toxicity tests [7,8]. In Japan for instance, the Ministry of Health and Welfare specified the TBC level to be lower than 20 μg/L in tap water [9]. The search to find a simple and efficient method to remove TBC from water is still ongoing and will definitely help in reducing the environmental problems that result from its current applications.

Recent years have witnessed the development of innovative technologies for water treatment technologies and removal of organic residues such as the advanced oxidation processes (AOPs) [10]. In essence, photocatalytic processes [11,12] using semiconductors that can generate reactive hydroxyl radicals upon exposition to UV–vis radiation have been thoroughly investigated. Titanium dioxide (TiO_2), as one of the most applied photocatalysts, has been successfully implemented to degrade thiobencarb [13,14]. However, the major drawback of this catalyst is its absorption of ultraviolet light only at wavelengths below 387.5 nm, which accounts for about 4% of sun-

* Corresponding author.
Email address: cslu6@nutc.edu.tw (C. Lu)

https://doi.org/10.1016/j.seppur.2018.01.009
Received 8 September 2017; Received in revised form 24 December 2017; Accepted 3 January 2018
Available online xxx
1383-5866/

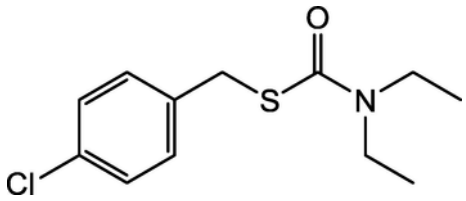

Fig. 1. Chemical structure of thiobencarb.

light. Thus, the photocatalytic activity of TiO_2 is low under visible light limiting its utility in the removal of organic molecules that requires high energy especially at a large scale [15,16].

In our previous studies, we have demonstrated the efficient degradation of thiobencarb using a visible light-driven monoclinic $BiVO_4$ catalyst [17]. $BiVO_4$ is found to be stable during 3 successive runs achieving a TBC removal level of 97% within 5 h. Nonetheless, the addition of hydrogen peroxide is indispensable to establish a prominent photocatalytic activity of $BiVO_4$. Hydroxyl radicals are only generated in considerable amount on $BiVO_4$ if H_2O_2 is added; else it is below the blank level [18]. There exist many studies that evaluate the economical and technical feasibility of treatment processes from all perspectives including the usage of additives. Therefore, the costly H_2O_2 is a major drawback that restricts the employment of $BiVO_4$ in large-scale treatments of water-soluble pesticides. In addition, the presence of anions has a dramatic effect on the catalytic activity of $BiVO_4$. In this study, we setup to find a suitable photocatalyst that operates effectively in the photodegradation of thiobencarb using only visible light irradiation without the need of any additives such as H_2O_2.

Molybdenum disulfide (MoS_2) has captivated large attention since it possesses exceptional features like large surface area and catalytically active sites [19,20]. MoS_2 has found important applications in different domains including hydrogen evolution reaction, hydrodesulfurization, and photocatalytic degradation of organic pollutants [21]. MoS_2 is characterized by a narrow band gap that allows the absorption of visible light and generation of electron–hole pairs upon excitation [22,23]. This attribute has made MoS_2 a potential candidate for photocatalytic applications under visible light. The photooxidation activity of MoS_2 nanoclusters and their catalytic role in the photolysis of organic molecules using visible light were first reported by Thurston et al. [24]. The higher utilization of solar radiation for nano MoS_2 announces it as an attractive alternative to TiO_2. James et al. [25] realized MoS_2 nanoparticles *via* thermal decomposition method and tested them in photocatalytic degradation of methylene blue bringing about an efficiency of 30%. Hu et al. [26] investigated the activity of nano-slice, nano-ball, and bulk MoS_2 in the photodecomposition of methyl orange using visible light. They found that the best photocatalytic activity was accomplished with MoS_2 nano-slice attaining a decomposition ratio greater than 90% after 2 h. Sheng et al. [27] studied the influence of excess sulfur source on the photocatalytic behavior of MoS_2 spheres and found that increasing the stoichiometric ratio of S/Mo by more than 2 led to enhance the photocatalytic activities.

As far as we know, the degradation of thiocarbamate herbicides using a MoS_2 photocatalyst has not been yet explored. Little knowledge can be *hitherto* obtained regarding the usability of MoS_2 in the treatment of thiobencarb in aqueous medium. Herein, the optimization of MoS_2 photocatalytic degradation of thiobencarb is described including systematic studies of the influence of various parameters (dosage, pH, effects of anions). Secondly, the dominant reactive species in this TBC photocatalytic decomposition are identified using experiments engaging the addition of different scavengers. Thirdly, the mechanism of the photodegradation of TBC in the MoS_2/visible light process is proposed by assigning the intermediates of this reaction. Lastly, this work investigates the recyclability and the potential of MoS_2 photocatalysis for practical applications in treatment of environmental water samples.

2. Experimental

2.1. Material

Thiobencarb was obtained from Sigma-Aldrich (99.8?) and used without further purification. Stock solution containing 5 mg L^{-1} of TBC in water was prepared, protected from light, and stored at 4 °C. HPLC analysis was employed to confirm the presence of TBC as a pure organic compound. Sodium molybdate $Na_2MoO_4{\cdot}2H_2O$ (Sigma, 99.5%) and L-cysteine (Alfa Aesar, 98%) were used as the molybdenum and sulfur sources of the MoS_2 catalyst. Reagent-grade ammonium acetate, sodium hydroxide, nitric acid, and HPLC-grade methanol were purchased from Merck. De-ionized water was used throughout this study. The water was purified with a Milli-Q water ion-exchange system (Millipore Co.) to give a resistivity of $1.8\times10^7\,\Omega$cm.

2.2. Preparation and characterization of MoS_2

For the synthesis of MoS_2 catalyst, 5 g of L-cysteine was dissolved in 40 mL distilled water under magnetic stirring at room temperature. Then 40 mL of sodium molybdate (1.2 g) solution was added to the L-cysteine solution under vigorous stirring for 30 min. The obtained slurry was then transferred into Teflon-lined stainless steel autoclave and heated to 180 °C for 24 h. After being naturally cooled to room temperature, the obtained precipitate was collected by filtration, washed with absolute ethanol and distilled water several times, and dried at 60 °C for 12 h.

X-ray powder diffraction (XRD) pattern was recorded on a PHILIPS X'PERT Pro MPD X-ray diffractometer with Cu Kα radiation, operated at 40 kV and 80 mA. Field emission scanning electron microscopy (FE-SEM) measurement was carried out with a field-emission microscope (HITACHI S-4800) at an acceleration voltage of 15 kV. An HRXPS measurement was performed with VG Scientific ESCALAB 250 XPS. The Al Kα radiation was generated with a voltage of 15 kV. The peak position of each element was corrected by C1s (284.6 eV).

2.3. Apparatus and instruments

The apparatus for studying the photocatalytic degradation of TBC has been described elsewhere [28]. The C-75 Chromato-Vue cabinet of UVP provides a wide area of illumination from the 4 W visible-light tubes positioned on two sides of the cabinet interior. A Waters LC system, equipped with a binary pump, an autosampler, and a photodiode array detector, was used for determining the amount of TBC in the aqueous solution. Solid-phase microextraction (SPME) and gas chromatography/mass spectrometry (GC/MS) were utilized for the analysis of intermediate products resulted from the photocatalytic degradation process. SPME holder and fiber-coating divinylbenzene-carboxen-polydimethylsiloxane (DVB-CAR-PDMS 50/30 μm) were supplied from Supelco (Bellefonte, PA). GC/MS analyses were run on a Perkin-Elmer AutoSystem-XL gas chromatograph interfaced to a TurboMass selective mass detector.

2.4. Procedures and analysis

TBC solution (5 mg L^{-1}) with the appropriate amount of photocatalyst was mixed and used in photocatalytic experiments. For reactions in different pH media, the initial pH of the suspension was adjusted by adding either NaOH or HNO_3 solution. Prior to irradiation, the suspension was magnetically stirred in the dark at room temperature for ca. 30 min to ensure the establishment of the adsorption/desorption equilibrium. Irradiation was carried out using two visible lamps (F4T5/CW, Philips Lighting Co.). The lamp mainly provides visible light in the range of 400–700 nm. The average light intensity striking the surface of the reaction solution was about 1420 lx, as

measured by a digital luxmeter. At the given irradiation time intervals, a 5 mL aliquot was collected and centrifuged to withdraw the MoS_2 catalyst. The amount of the TBC residual was thus determined by HPLC. Two types of eluents were employed in this study: 0.025 M ammonium acetate (solvent A) and methanol (solvent B). LC was carried out on an Atlantis™ dC_{18} column (250 mm × 4.6 mm i.d., dp = 5 μm). The flow rate of the mobile phase was set at 1 mL/min. A linear gradient was run as follows, $t = 0$, $A = 95$, $B = 5$; $t = 20$, $A = 50$, $B = 50$; $t = 35$–40, $A = 10$, $B = 90$; and, $t = 45$, $A = 95$, $B = 5$. The elution was monitored at 220 nm.

SPME-GC/MS was used for identifying the reaction intermediates. The SPME fiber was directly immersed into the sample solution to extract TBC and its intermediates for 30 min at room temperature, with magnetic stirring at 550 ± 10 rpm on the Corning stirrer/plate (Corning, USA). Finally, the compounds were thermally desorbed from the fiber to the GC injector for 45 min. Separation was carried out in a DB-5 capillary column (5% diphenyl/95% dimethyl-siloxane), 60 m, 0.25-mm i.d., and 1.0-μm thick film. A split-splitless injector was used under the conditions of injector temperature 250 °C and split flow 10 mL/min. The helium carrier gas flow was 1.5 mL/min. The oven temperature was programmed at 60 °C for 1.0 min then increased at 8 °C min^{-1} until reaching 240 °C. It was kept at this temperature for 21.5 min, and the total run time was 45 min. Electron impact mass spectra were obtained at 70 eV of electron energy and monitored from 20 to 350 *m/z*. The ion source and inlet line temperatures were set at 220 and 250 °C, respectively.

2.5. Procedure for degradation of thiobencarb in real samples

In order to investigate the efficiency of MoS_2 photocatalysis system in the real natural water solution, river water was collected from the Han River in Taichung city and lake water was collected from the lake in Taichung Park. All samples were filtered through a 0.45 μm membrane for the removal of suspended solids and stored in the dark at 4 °C until analysis. Finally, the real water samples were spiked with the target compound (at 5 mg L^{-1}) just prior to photocatalytic experiments. Degradations were performed on 100 mL of real water samples containing 1.0 g L^{-1} MoS_2 at pH 6.5.

3. Results and discussion

3.1. Characterization of MoS_2

In this paper, the MoS_2 microsphere was hydrothermally prepared with the assistance of L-cysteine, a common amino acid and an environmentally benign sulfur source. Besides, the MoS_2 microsphere was obtained at lower temperature (180 °C) and shorter time (24 h) to reduce the energy consumption. Table 1 summarizes the recent related papers collected for MoS_2 [21,29–37]. In these literatures, a hydrothermal reaction of sodium molybdate with thiourea, thioacetamide, or cysteine is carried out at 200–240 °C for 24–48 h.

The X-ray diffraction pattern for MoS_2 powder obtained *via* the hydrothermal method is displayed in Fig. 2. The observed diffraction peaks at $2\theta = 14.4°$, 32.5° and 58.0° can be well attributed to the (0 0 2), (1 0 0), and (1 1 0) planes of hexagonal MoS_2 (JCPDS No. 37-1492), respectively. No other impurity peak is observed in the spectrum, implying a high purity of the fabricated MoS_2 structure. This result is in good agreement with previous reports [29,38]. Fig. 3 shows the morphology of the synthesized MoS_2 powder under a field-emission SEM microscope. It can be seen that the MoS_2 products are irregular microspheres with rough surfaces and the mean diameter of the spheres is around 500 nm. Close observation indicates that these microspheres consist of many crossed-linked nanorods with length around 100 nm. The composition of the MoS_2 powder and the valence state of Mo and S were verified using XPS spectra (Fig. 4). The peaks located at 232.8 and 228.6 eV are Mo $3d_{3/2}$ and Mo $3d_{5/2}$ binding energies, respectively. These peaks can be attributed to the Mo ion species with +4 oxidation state. In Fig. 4b, S 2p spectrum primarily showed a strong XPS peak at 162.8 eV, which corresponds to S^{2-} ion in the MoS_2. All the binding energies are conformed to the values previously reported for MoS_2 crystals [39,40].

Table 1
Summary of recent related papers collected for MoS_2.

	Sodium molybdate	Sulfur source[a]	pH	Reaction temperature	Reaction time	Use	Reference
This study	5 mmol	CYS 40 mmol	7	180 °C	24 h	Photocatalyst	
Chen et al.	1.5 mmol	CYS 4.5 mmol	< 1	240 °C	24 h	–	[29]
Park et al.	6 mmol	CYS 25 mmol	1	220 °C	36 h	Li-ion storage	[30]
Huang et al.	1 mmol	CYS 3 mmol	6.5	180 °C	48 h	Supercapacitor electrode	[31]
Wang et al.	1.25 mmol	CYS 10 mmol	–	220 °C	24 h	Supercapacitor electrode	[32]
Zhou et al.	2 mmol	TAA 10 mmol	–	240 °C	24 h	Photocatalyst MB	[21]
Guo et al.	1 mmol	TAA 8 mmol	0.5 mmol oxalic acid	200 °C	24 h	Hydrogen evolution	[33]
Patel et al.	0.124 mmol	TAA 0.80 mmol	–	200 °C	24 h	Energy storage	[34]
Feng et al.	4 mmol	TU 15 mmol	3 mmol oxalic acid	200 °C	24 h	–	[35]
Kim et al.	2.77 mmol	TU 11.1 mmol	–	210 °C	24 h	–	[36]
Sun et al.	7 mmol	TU 35 mmol	< 1	200 °C	24 h	N_2 reduction	[37]

[a] Sulfur source: L-cysteine (CYS); thiourea (TU); thioacetamide (TAA).

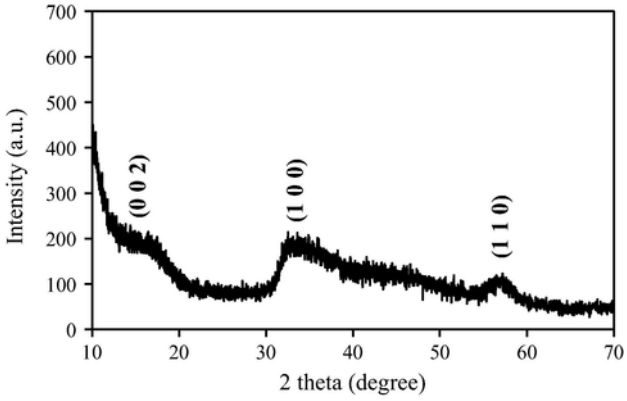

Fig. 2. XRD pattern of the as-prepared MoS_2 photocatalyst.

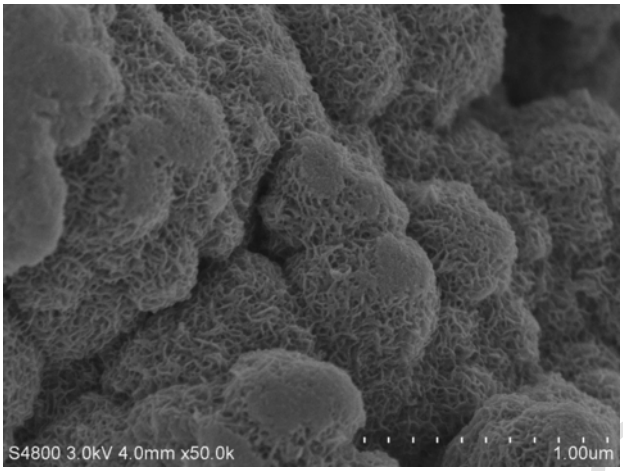

Fig. 3. SEM image of the as-prepared MoS_2 photocatalyst.

3.2. Photocatalytic reaction

3.2.1. Effect of catalyst dosage on the degradation of TBC

The dosage of the photocatalyst is a critical parameter that decides the photodegradation of organic compounds. Thus, we have performed an optimization study using different concentrations of MoS_2 ranging from 0.25 to 1.5 g L^{-1} to examine the effect of MoS_2 concentration on the rate of TBC degradation. The negligible degradation of TBC under visible-light irradiation in the absence of the catalyst (up to 16 h) evidences the important role of MoS_2 in the photodegradation of this organic compound (Fig. 5). The rate of the TBC photocatalytic degradation increased with increasing the MoS_2 dosage up to a concentration of 1.0 g L^{-1}. After this optimal dosage, the reaction rate was slightly decreased. The observed faster degradation with increasing the MoS_2 dosage is related to the increase in the total surface area (or number of accessible active sites) available for the photocatalytic reaction. Overdosing MoS_2 after the optimal concentration causes less penetration and more scattering of the incident light, which counteracts the favorable increment in the catalytic surface area, and hence the overall rate of the photodegradation is decreased [41].

3.2.2. Effect of initial pH value on the degradation of TBC

Another principal parameter that can dramatically compromise photocatalytic activity is the initial pH. Investigating the effect of the initial pH value on the rate of TBC decomposition for the MoS_2 suspensions is presented in Fig. 6. These experiments have shown that TBC can be degraded perfectly at pH value of 6–9 of the TBC solution. However, the photodegradation rate decreases rapidly with the pH value decreasing from 6 to 3, the

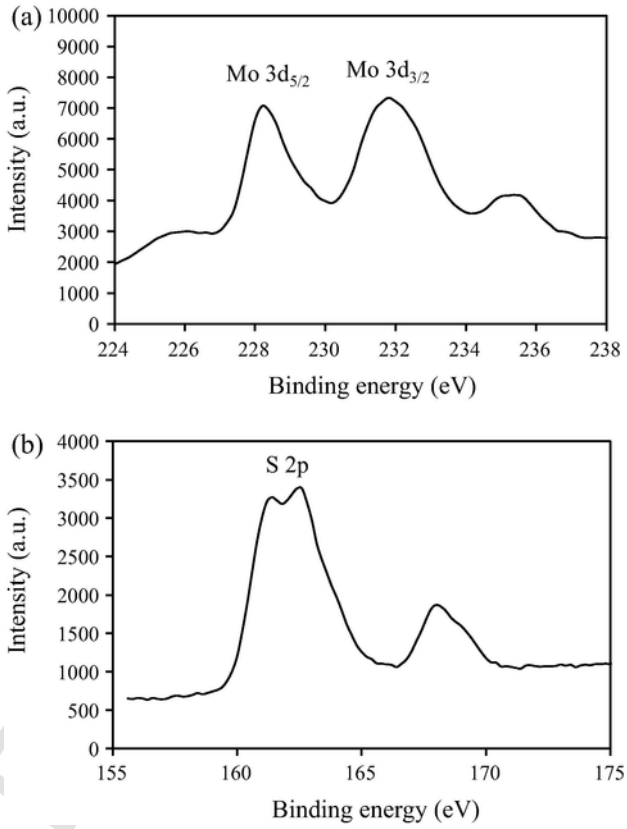

Fig. 4. XPS spectra of the as-prepared MoS_2 photocatalyst: (a) Mo 3d; (b) S 2p.

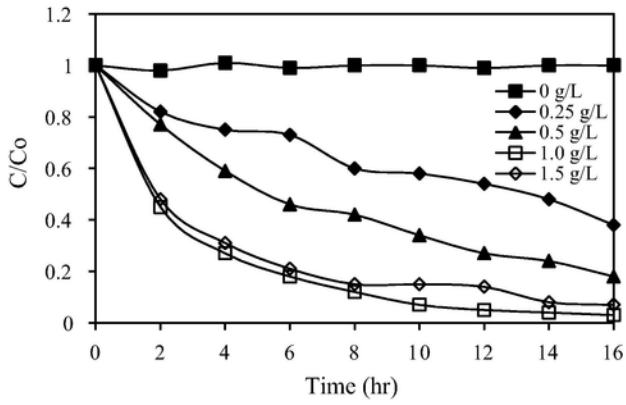

Fig. 5. Effect of MoS_2 dosage on the photocatalytic degradation rate of TBC. Experimental conditions: TBC concentration 5 mg L^{-1}; pH 6.5.

degradation of TBC is difficult to occur in acidic solution. The surface charge of a semiconductor is affected by pH and is a key factor that influences the electrostatic interactions with the substrate (neutral, anionic, or cationic). These interactions, in turn, either enhance or inhibit the photodegradation rate of the substrate [42]. Since TBC is initially present in a neutral form, the rate enhancement of its photodegradation in an alkaline medium is most likely associated to the increased hydroxylation of the photocatalyst as a result of the large concentration of hydroxide ions. This also leads to the formation of a higher concentration of $^{\bullet}OH$ free radicals, which are the major oxidizing species in this photodegradation reaction (*vide infra*). Thus, TBC photodecomposition is accelerated in an alkaline medium. In contrast, the catalyst surface is positively charged in an acidic medium and the concentration of the hydroxide ions (and hence the hydroxyl active species) is very low, which significantly decrease the degradation efficiency.

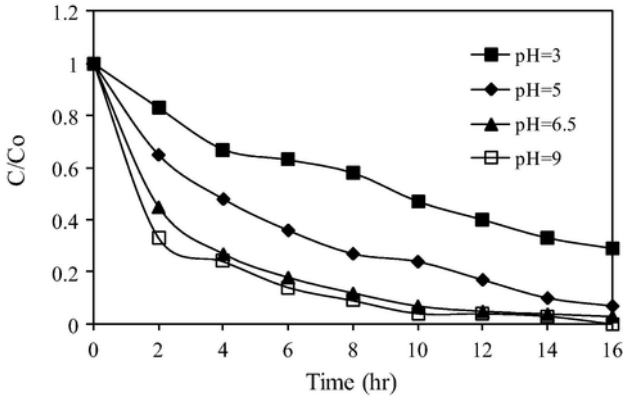

Fig. 6. pH effect on the photocatalytic degradation rate of TBC. Experimental conditions: TBC concentration 5 mg L^{-1}; MoS_2 concentration 1 g L^{-1}.

A similar effect of pH on the photocatalytic reaction has been reported for the degradation of methylene blue using a MoS_2 photocatalyst [43].

3.2.3. Effects of anions on the degradation of TBC

The presence of anions is rather common in aqueous environment. Thus, the inspection of how different anion species affect the photodegradation of TBC is crucial. The impact of chloride and nitrate ions on the rate of TBC decomposition was tested by respectively adding NaCl and $NaNO_3$ to the suspension to obtain a solution containing 0.05 M of Cl^- and NO_3^- ions before the beginning of irradiation. The degradation efficiency reached 85% and 80% after 12 h in the presence of Cl^- and NO_3^- respectively, showing a minimal effect on the photocatalytic activity of MoS_2 (Fig. 7). This is an additional advantage in favor of the usage of MoS_2 in water treatment as compared to $BiVO_4$ where Cl^- species reduces the photodegradation efficiency to around 40% [17]. The slightly prolonged reaction time can be explained as the anions may act as scavengers for the active species (hydroxyl radicals ($^{\bullet}OH$) and positive holes (h^+)) in this reaction (Eqs. (1) and (2). Although the generated radicals ($ClOH^{-\bullet}$ for instance) may have a considerable reactivity, they are less reactive than h^+ and $^{\bullet}OH$, and hence they slightly reduce the rate of photocatalytic degradation [44,45].

$$Cl^- + h^+ \rightarrow Cl^{\bullet} \quad (1)$$

$$Cl^- + {}^{\bullet}OH \rightarrow ClOH^{-\bullet} \quad (2)$$

3.2.4. Detection of active species by scavengers

Different scavengers have been introduced into the TBC/MoS_2 system in order to identify the nature of the active species ($HO^{\bullet}$, h^+, $^{\bullet}O_2^-$, etc.) playing a role in this photocatalytic reaction. Isopropanol (IPA), ammonium oxalate (AO), and 1,4-benzoquinone (BQ) are used as the scavengers for $HO^{\bullet}$, h^+, $^{\bullet}O_2^-$ respectively [46]. The photocatalytic degradation of thiobencarb with the MoS_2 catalyst in the presence and absence of the three scavengers under visible-light irradiation is displayed in Fig. 8. The addition of BQ slightly changes the degradation pattern of TBC, which eliminates the hypothesis that $^{\bullet}O_2^-$ can be a major reactive species in this photocatalytic oxidation. On the contrary, adding IPA and AO seriously decreases the TBC degradation efficiency, implying that hydroxyl radicals and photogenerated holes represent the major reactive species in the photocatalytic oxidation process.

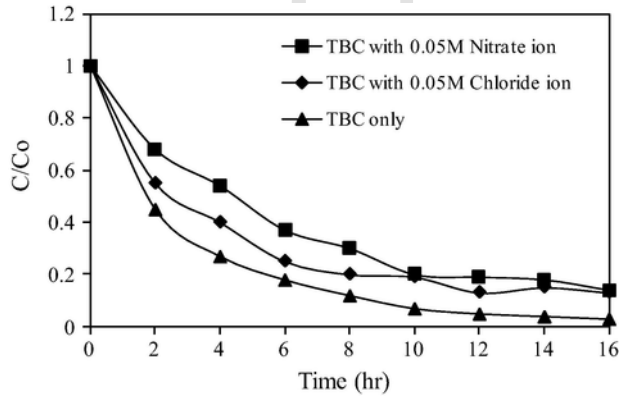

Fig. 7. Effect of anions on the photocatalytic degradation rate of TBC. Experimental conditions: TBC concentration 5 mg L^{-1}; MoS_2 concentration 1 g L^{-1}; pH 6.5.

3.2.5. Reaction pathway of TBC degradation

Besides the catalytic behavior of MoS_2 in TBC removal, it is important to elaborate the formation of the intermediate products and to conclude a plausible mechanism for this reaction. SPME-GC/MS technique was applied to identify the intermediates during the photodegradation of TBC. Fig. 9 shows the chromatogram of the MoS_2-treated solution after irradiation for 8 h. The peak at 33.61 min was the starting material (TBC). The major peaks were labeled as **I–IV**. Minor peaks were barely noticed; their intensities were not sufficient to elucidate their mass fragmentation, suggesting that they are less significant in this degradation pathway. Peaks **I–VI** increased firstly and then decreased subsequently, confirming the generation and consecutive transformation of the intermediates. Table 2 summarizes the detected intermediates of TBC, their retention times, and their characteristic ions of the mass spectra. As discussed before, h^+ and $^{\bullet}OH$ are the dominant reactive species in this process. These radical species are known to be nonselective radicals that can attack different reactive sites of the substrate, which is in line with a number of TBC degradation products.

Based on the identified intermediates, the mechanism of TBC photodegradation is proposed in Fig. 10. It comprises three different pathways, which correspond to the three possible reactive sites on the TBC molecule. These routes are consistent with our previously reported mechanism using $BiVO_4$ [17]. The first possible degradation route involves the initial attack of the aromatic ring by a hydroxyl radical forming the ring-hydroxylated product (**I**). Indeed, it is well documented that hydroxyl free radicals ($HO^{\bullet}$) undergo aromatic hydroxylation as a typical reaction, where the electrophilic nature of the $HO^{\bullet}$ radicals allows the preferential attack on the aromatic ring, forming the hydroxycyclohexadienyl radical intermediate. Further oxidation of the radical intermediate by molecular oxygen generates the phenolic product (**I**) [47].

Concerning the N-dealkylation route, the $HO^{\bullet}$ radical electrophiles can act on the C—H bonds adjacent to nitrogen, known for the pronounced stereoelectronic effect, which enhances the rate of abstraction of the hydrogen atom. Thus, carbon-centered radicals can be formed via the ab-

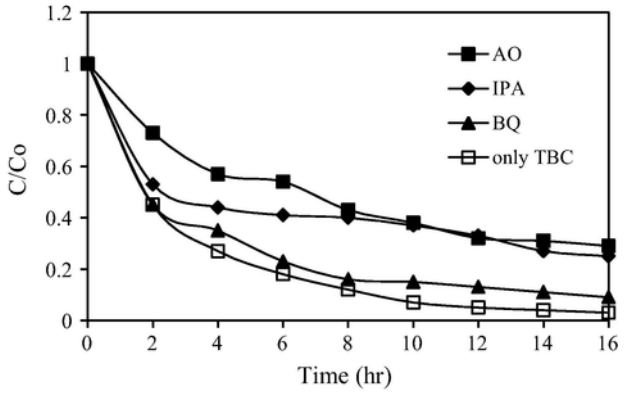

Fig. 8. Photocatalytic degradation of thiobencarb with MoS_2 catalyst in the absence and presence of scavengers (IPA, AO, and BQ) under visible-light irradiation. Experimental conditions: TBC concentration 5 mg L^{-1}; MoS_2 concentration 1 g L^{-1}; scavenger concentration 1×10^{-3} M; pH 6.5.

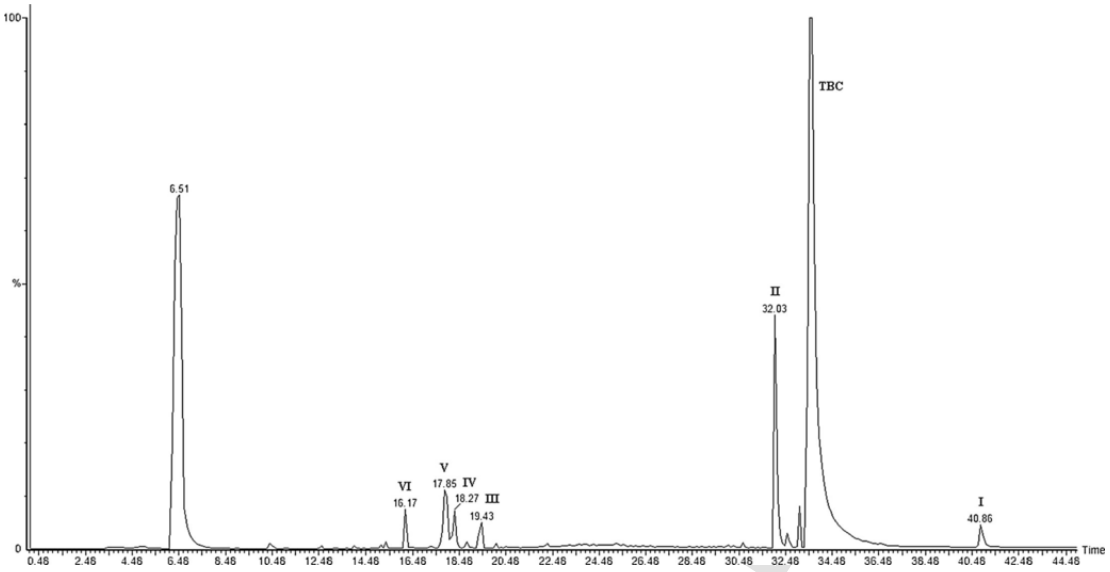

Fig. 9. GC/MS chromatogram obtained for TBC solution (100 mg L^{-1}) after 8 h of irradiation with visible light in the presence of MoS_2 (1 g L^{-1}).

Table 2
Identification of the intermediates from the photodegradation of thiobencarb by GC/MS.

Peaks	Photodegradation intermediates	R.T. (min)	MS peaks (*m/z*)
I	S-4-chloro-2/3-hydroxybenzyl diethylthiocarbamate	40.86	273, 141, 100, 72, 44, 29
TBC	S-4-chlorobenzyl diethylthiocarbamate	33.61	257, 125, 100, 72, 44, 29
II	S-4-chlorobenzyl ethylthiocarbamate	32.03	229, 158, 125, 89, 72
III	4-chlorobenzyl mercaptan	19.43	158, 125, 89, 63, 45
IV	4-chlorobenzyl alcohol	18.27	142, 107, 79, 77, 51
V	4-chloro-2/3-hydroxybenzaldehyde	17.85	156, 155, 99, 63, 39
VI	4-chlorobenzaldehyde	16.17	140, 139, 111, 75, 50

straction of the α-hydrogen atoms of ethylamine group prone to radical attack. In addition, the reaction of the radicals with the lone-pair electron of the nitrogen atom can produce a cationic radical that subsequently converts to these carbon-centered radicals [48]. The oxygen addition to these generated radical form the peroxyl radicals, which decompose to compounds (**II**).

The third pathway is initiated by the oxidative cleavage of the C—S bond resulting in compounds (**III–VI**). This transformation takes place by the attack of positive holes on the TBC leading to its oxidation into a cation radical via a transfer of a single electron from the S atom. Cation radicals have previously been reported in the degradation of thioethers [49] and organophosphorus pesticides [50]. The generated cation radical can undergo a scission of the C—S bond forming $ClC_6H_4CH_2S^{\bullet}$ radical as a precursor of compound (**III**). As shown earlier by Kerzhentsev et al. [51], the proton reduction by photogenerated electron $H^{\pm} + e^{-} \rightarrow H^{\bullet}$ provides the hydrogen atom needed for the formation of the S—H bond in compound (**III**). Similarly, the scission of the C—S bond can generate (4-chlorophenyl)methylium ion, which is found to be unstable and rapidly hydrolyzed to form 4-chlorobenzyl alcohol (**IV**). Compound (**IV**) is subsequently oxidized into 4-chlorobenzaldehyde (**VI**) and 4-chloro-2/3-hydroxybenzaldehyde (**V**).

3.2.6. Performance of recycled catalyst

As we know, it is essential to assess the stability and reusability of a photocatalyst. The circulating runs in the photocatalytic oxidation of TBC under visible-light irradiation were carried out to evaluate these factors. The MoS_2 catalyst was collected after each run, dried, and reused under the same experimental conditions. It could be observed that MoS_2 did not show any loss of catalytic activity in 3 successive runs (Fig. 11). In summary, this finding demonstrates that MoS_2 photocatalyst exhibits excellent stability and reusability without encountering a photocorrosion effect during the photocatalytic reaction, which favors its long-term utilization in the removal of organic pollutants.

3.2.7. Photocatalytic process of real water samples

For application purposes, there is a need to investigate the MoS_2 photocatalysis in the removal of thiobencarb from real water sample under visible-light illumination. Fig. 12 illustrates the comparison of the TBC photodegradation rates in deionized, river, and lake water. In the real water samples, the TBC concentration in MoS_2 photocatalysis decreased with the increase of irradiation time, confirming the catalytic activity of the prepared photocatalyst. The degradation rate of thiobencarb in real water samples was slightly decreased as compared to that in deionized water. This decrease might arise from the presence of some anions (Table 3) in real water acting as scavengers of the active radical species. Nevertheless, the results validate the photocatalytic activity of MoS_2 in the degradation of TBC in real water samples, affirming the potential of this catalyst in the actual treatment of contaminated wastewater and the environmental water samples.

4. Conclusions

MoS_2 microspheres have been synthesized by the hydrothermal method using sodium molybdate and L-cysteine as the source materials. Thiobencarb could be successfully degraded in a MoS_2 suspension under visible-light irradiation and without the addition of hydrogen peroxide. At optimal operating parameters, its degradation efficiency could reach 95% in 12 h. The photodegradation rate of TBC was found to increase with increasing the pH to 6–9 value and with increasing the catalyst concentration until reaching the optimal dosage of 1.0 g L^{-1}. Moreover, the presence of inorganic ions such as chloride and nitrate that are often found in natural water induced a

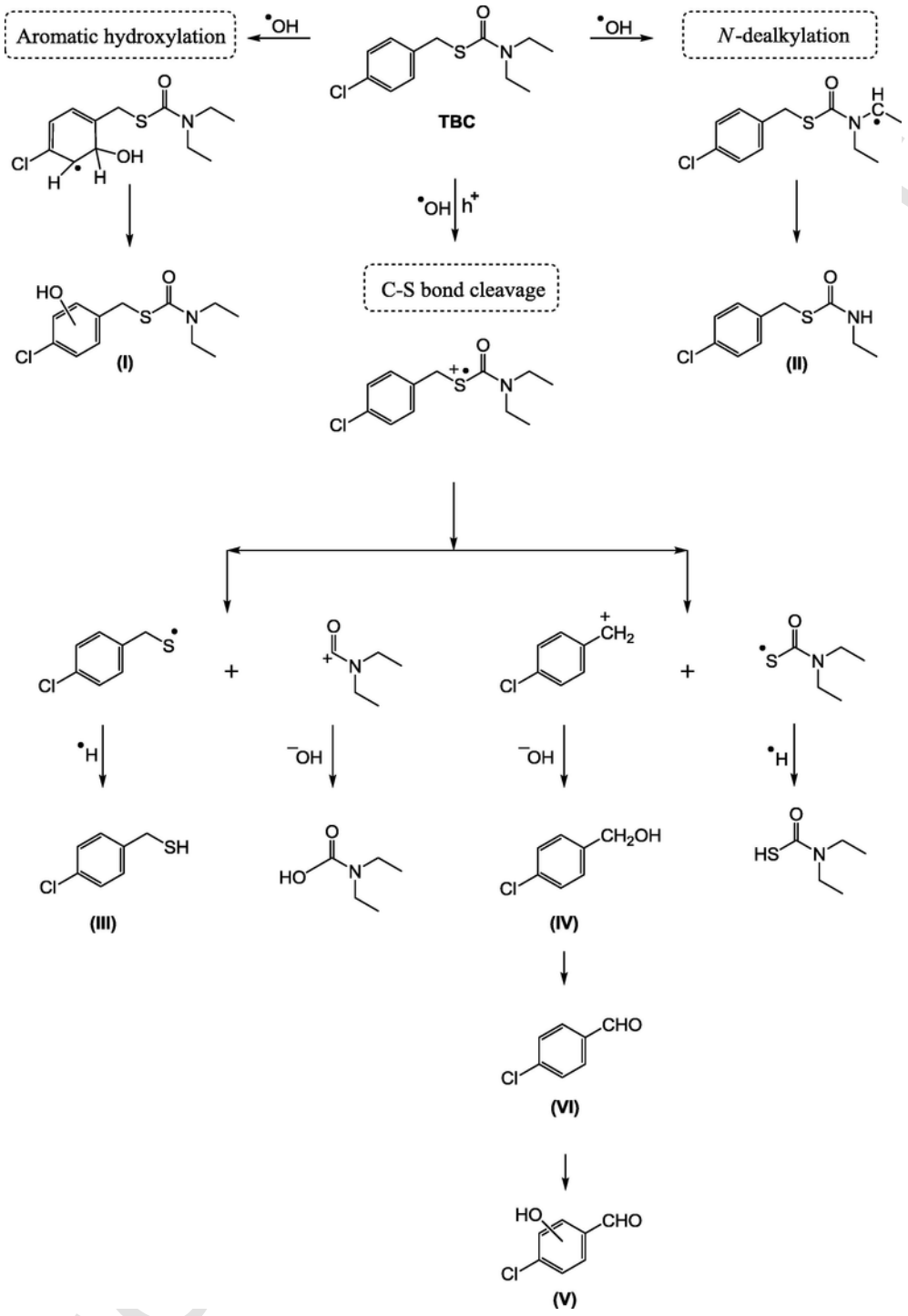

Fig. 10. Proposed photodegradation mechanism of the thiobencarb followed by the identification of several intermediates by GC/MS technique.

minor effect on the degradation efficiency. The scavenger tests conclude that hydroxyl radicals and holes are the major active species contributing to this photodegradation. The main intermediates of the degradation process were described and characterized by GC/MS technique. The intermediates suggest that dealkylation, hydroxylation, and C—S bond cleavage are three possible transformations in TBC degradation. The catalyst proved to be remarkably stable and reusable in three successive runs without any significant loss in its photocatalytic activity. Finally, the application of the MoS_2 photocatalyst in TBC degradation from environmental water samples (lake and river water) was carried out, demonstrating its prospect in water treatment.

Acknowledgment

This research was supported by the Ministry of Science and Technology of the Republic of China (MOST 105-2113-M-025-001).

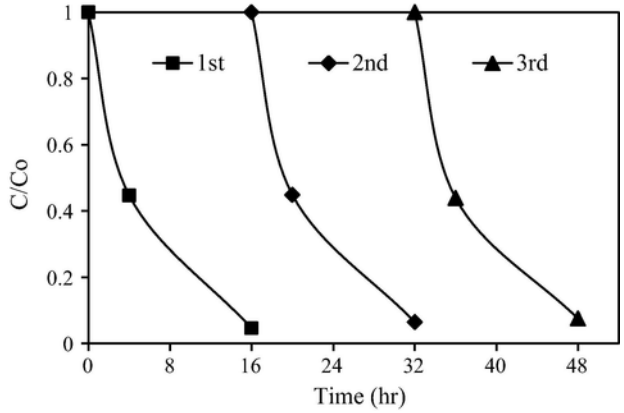

Fig. 11. Cycling runs in the photocatalytic degradation of TBC with MoS_2 catalyst under visible-light irradiation.

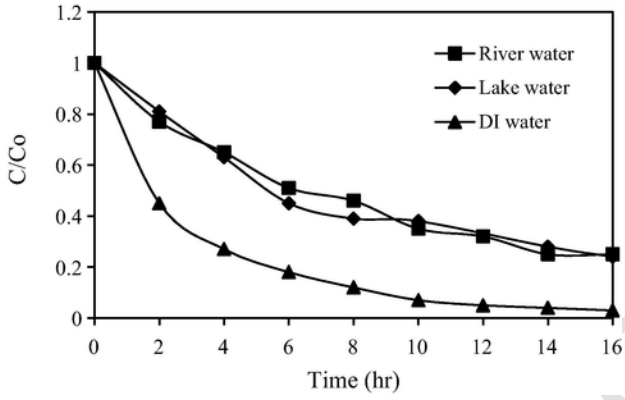

Fig. 12. Photocatalytic degradation rates of thiobencarb in deionized and real water samples. Experimental conditions: MoS_2 concentration, 1 g L^{-1}; pH 6.5.

Table 3
Characteristics of the real water sample.

Parameter	River water	Lake water
pH	6.30	6.24
Conductivity (μmho cm^{-1})	420	378
Turbidity (NTU)	2.9	4.9
Sulfate (mg L^{-1})	48.1	50.9
Chloride (mg L^{-1})	22.6	16.7
Nitrate (mg L^{-1})	84.8	2.9
Nitrite (mg L^{-1})	1.12	0.02

References

[1] J. Zhang, S.-S. Liu, J. Zhang, L.-T. Qin, H.-P. Deng, Two novel indices for quantitatively characterizing the toxicity interaction between ionic liquid and carbamate pesticides, J. Hazard. Mater. 239–240 (2012) 102–109.

[2] S. Bogialli, R. Curini, A.D. Corcia, A. Laganà, M. Nazzari, M. Tonci, Simple and rapid assay for analyzing residues of carbamate insecticides in bovine milk: hot water extraction followed by liquid chromatography–mass spectrometry, J. Chromatogr. A 1054 (2004) 351–357.

[3] J.M.F. Nogueira, T. Sandra, P. Sandra, Considerations on ultra trace analysis of carbamates in water samples, J. Chromatogr. A 996 (2003) 133–140.

[4] US Environmental Protection Agency, National Survey of Pesticides in Drinking Water Wells, Phase II Report, EPA 570/9-91-020, National Technical Information Service, Springfield, VA, 1992.

[5] Q. Wu, Q. Chang, C. Wu, H. Rao, X. Zeng, C. Wang, Z. Wang, Ultrasound- assisted surfactant-enhanced emulsification microextraction for the determination of carbamate pesticides in water samples by high performance liquid chromatography, J. Chromatogr. A 1217 (2010) 1773–1778.

[6] S.N. Pentyala, C.S. Chetty, Comparative studies on the changes in AChE and ATPase activities in neonate and adult rat brains under thiobencarb stress, J. Appl. Toxicol. 13 (1993) 39–42.

[7] H. Jinno, N. Hanioka, A. Takahashi, T. Nishimura, T. Toyo'oka, M. Ando, Comparative cytotoxicity of the aqueous chlorination products of thiobencarb, a thiocarbamate herbicide, in cultured rat hepatocytes, Toxicol. in Vitro 11 (1997) 731–739.

[8] S. Kodama, A. Yamamoto, A. Matsunaga, S-oxygenation of thiobencarb in tap water processed by chlorination, J. Agric. Food Chem. 45 (1997) 990–994.

[9] Md.N. Amin, S. Kaneco, T. Kato, H. Katsumata, T. Suzuki, K. Ohta, Removal of thiobencarb in aqueous solution by zero valent iron, Chemosphere 70 (2008) 511–515.

[10] M.A. Oturan, J.-J. Aaron, Advanced oxidation processes in water/wastewater treatment: principles and applications. A review, Crit. Rev. Environ. Sci. Technol. 44 (2014) 2577–2641.

[11] I. Losito, A. Amorisco, F. Palmisano, Electro-Fenton and photocatalytic oxidation of phenyl-urea herbicides: an insight by liquid chromatography– electrospray ionization tandem mass spectrometry, Appl. Catal. B: Environ. 79 (2008) 224–236.

[12] Y.S. Wu, C.C. Chen, Y.C. Huang, W.Y. Lin, Y.T. Yen, C.S. Lu, Pirimicarb degradation by $BiVO_4$ photocatalysis: parameter and reaction pathway investigations, Sep. Sci. Technol. 51 (2016) 2284–2296.

[13] H.F. Lai, C.C. Chen, R.J. Wu, C.S. Lu, Thiobencarb degradation by Ti_{O2} photocatalysis: parameter and reaction pathway investigations, J. Chin. Chem. Soc. 59 (2012) 87–97.

[14] M. Sturini, E. Fasani, C. Prandi, A. Casaschi, A. Albini, Titanium dioxide- photocatalysed decomposition of some thiocarbamates in water, J. Photochem. Photobiol. A: Chem. 101 (1996) 251–255.

[15] C.Y. Wang, H. Zhang, F. Li, L.Y. Zhu, Degradation and mineralization of bisphenol A by mesoporous Bi_2WO_6 under simulated solar light irradiation, Environ. Sci. Technol. 44 (2010) 6843–6848.

[16] H. Zhang, P. Zhang, Y. Ji, J. Tian, Z. Du, Photocatalytic degradation of four non-steroidal anti-inflammatory drugs in water under visible light by P25-TiO_2/tetraethyl orthosilicate film and determination via ultra performance liquid chromatography electrospray tandem mass spectrometry, Chem. Eng. J. 262 (2015) 1108–1115.

[17] H.-F. Lai, C.-C. Chen, Y.-K. Chang, C.-S. Lu, R.-J. Wu, Efficient photocatalytic degradation of thiobencarb over $BiVO_4$ driven by visible light: parameter and reaction pathway investigations, Sep. Purif. Technol. 122 (2014) 78–86.

[18] T. Saison, N. Chemin, C. Chanéac, O. Durupthy, L. Mariey, F. Maugé, V. Brezová, J.-P. Jolivet, New insights into $BiVO_4$ properties as visible light photocatalyst, J. Phys. Chem. C 119 (2015) 12967–12977.

[19] D. Kong, H. Wang, J.J. Cha, M. Pasta, K.J. Koski, J. Yao, Y. Cui, Synthesis of MoS_2 and $MoSe_2$ films with vertically aligned layers, Nano Lett. 13 (2013) 1341–1347.

[20] H.I. Karunadasa, E. Montalvo, Y. Sun, M. Majda, J.R. Long, C.J. Chang, A molecular MoS_2 edge site mimic for catalytic hydrogen generation, Science 335 (2012) 698–702.

[21] Z. Zhou, Y. Lin, P. Zhang, E. Ashalley, M. Shafa, H. Li, J. Wu, Z. Wang, Hydrothermal fabrication of porous MoS_2 and its visible light photocatalytic properties, Mater. Lett. 131 (2014) 122–124.

[22] Y. Yuan, P. Shen, Q. Li, G. Chen, H. Zhang, L. Zhu, B. Zou, B. Liu, Excellent photocatalytic performance of few-layer MoS_2/graphene hybrids, J. Alloy. Compd. 700 (2017) 12–17.

[23] M.Q. Wen, T. Xiong, Z.G. Zang, W. Wei, X.T. Tang, F. Dong, Synthesis of MoS_2/g-C_3N_4 nanocomposites with enhanced visible-light photocatalytic activity for the removal of nitric oxide (NO), Opt. Exp. 24 (2016) 10205–10212.

[24] T.R. Thurston, J.P. Wilcoxon, Photooxidation of organic chemicals catalyzed by nanoscale MoS_2, J. Phys. Chem. B 103 (1999) 11–17.

[25] D. James, T. Zubkov, Photocatalytic properties of free and oxide-supported MoS_2 and WS_2 nanoparticles synthesized without surfactants, J. Photochem. Photobiol. A 262 (2013) 45–51.

[26] K.H. Hu, X.G. Hu, Y.F. Xu, X.Z. Pan, The effect of morphology and size on the photocatalytic properties of MoS_2, React. Kinet. Mech. Catal. 100 (2010) 153–163.

[27] B. Sheng, J. Liu, Z. Li, M. Wang, K. Zhu, J. Qiu, J. Wang, Effects of excess sulfur source on the formation and photocatalytic properties of flower-like MoS_2 spheres by hydrothermal synthesis, Mater. Lett. 144 (2015) 153–156.

[28] C.C. Chen, C.S. Lu, F.D. Mai, C.S. Weng, Photooxidative N-de-ethylation of anionic triarylmethane dye (sulfan blue) in titanium dioxide dispersions under UV irradiation, J. Hazard. Mater. B 137 (2006) 1600–1607.

[29] X. Chen, H. Li, S. Wang, M. Yang, Y. Qi, Biomolecule-assisted hydrothermal synthesis of molybdenum disulfide microspheres with nanorods, Mater. Lett. 66 (2012) 22–24.

[30] S.-K. Park, S.-H. Yu, S. Woo, J. Ha, J. Shin, Y.-E. Sung, Y. Piao, A facile and green strategy for the synthesis of MoS_2 nanospheres with excellent Li-ion storage properties, CrystEngComm 14 (2012) 8323–8325.

[31] K.-J. Huang, J.-Z. Zhang, G.-W. Shi, Y.-M. Liu, Hydrothermal synthesis of molybdenum disulfide nanosheets assupercapacitors electrode material, Electrochim. Acta 132 (2014) 397–403.

[32] L. Wang, Y. Ma, M. Yang, Y. Qi, Hierarchical hollow MoS_2 nanospheres with enhanced electrochemical properties used as an Electrode in Supercapacitor, Electrochim. Acta 186 (2015) 391–396.

[33] B. Guo, K. Yu, H. Li, H. Song, Y. Zhang, X. Lei, H. Fu, Y. Tan, Z. Zhu, Hollow structured micro/nano MoS_2 spheres for highly electrocatalytic activity hydrogen evolution reaction, ACS Appl. Mater. Interfaces 8 (2016) 5517–5525.

[34] R. Patel, A.I. Inamdar, H.B. Kim, H. Im, H. Kim, In-situ hydrothermal synthesis of a MoS_2 nanosheet electrode for electrochemical energy storage applications, J. Kor. Phys. Soc. 68 (2016) 1341–1346.

[35] G. Feng, A. Wei, Y. Zhao, J. Liu, Synthesis of flower-like MoS_2 nanosheets microspheres by hydrothermal method, J. Mater. Sci.: Mater. Electron. 26 (2015) 8160–8166.

[36] J.H. Kim, J. Kim, S.D. Oh, S. Kim, S.-H. Choi, Sequential structural and optical evolution of MoS_2 by chemical synthesis and exfoliation, J. Kor. Phys. Soc. 66 (2015) 1852–1855.
[37] S. Sun, X. Li, W. Wang, L. Zhang, X. Sun, Photocatalytic robust solar energy reduction of dinitrogen toammonia on ultrathin MoS_2, Appl. Catal. B – Environ. 200 (2017) 323–329.
[38] X. Zhang, R. Ke, J. Wang, S. Zhang, H. Niu, C. Mao, J. Song, B. Jin, Y. Tian, Facile electrosynthesis and photoelectric conversion of Ag nanodendrites wrapped with MoS_2 nanosheets, Electrochim. Acta 188 (2016) 917–926.
[39] K.-J. Huang, L. Wang, J.-Z. Zhang, K. Xing, Synthesis of molybdenum disulfide/carbon aerogel composites for supercapacitors electrode material application, J. Electroanal. Chem. 752 (2015) 33–40.
[40] H. Liu, T. Lv, C. Zhu, X. Su, Z. Zhu, Efficient synthesis of MoS_2 nanoparticles modified TiO_2 nanobelts with enhanced visible-light-driven photocatalytic activity, J. Mol. Catal. A 396 (2015) 136–142.
[41] C.C. Wong, W. Chou, The direct photolysis and photocatalytic degradation of alachlor at different TiO_2 and UV sources, Chemosphere 50 (2003) 981–987.
[42] X. Zhu, C. Yuan, Y. Bao, J. Yang, Y. Wu, Photocatalytic degradation of pesticide pyridaben on TiO_2 particles, J. Mol. Catal. A 229 (2005) 95–105.
[43] M. Sabarinathan, S. Harish, J. Archana, M. Navaneethan, H. Ikeda, Y. Hayakawa, Controlled exfoliation of monodispersed MoS_2 layered nanostructures by ligand-assisted hydrothermal approach for the realization of ultrafast degradation of organic pollutant, RSC Adv. 6 (2016) 109495–109505.
[44] N.M. Mahmoodi, M. Arami, N.Y. Limaee, K. Gharanjig, Photocatalytic degradation of agricultural N-heterocyclic organic pollutants using immobilized nanoparticles of titania, J. Hazard. Mater. 145 (2007) 65–71.
[45] I.K. Konstantinou, T.A. Albanis, TiO_2-assisted photocatalytic degradation of azo dyes in aqueous solution: kinetic and mechanistic investigations, a review, Appl. Catal. B: Environ. 49 (2004) 1–14.
[46] Z. Yu, C. Dong, R. Qiu, L. Xu, A. Zheng, Photocatalytic degradation of methyl orange by $PbXO_4$ (X = Mo, W), J. Colloid Interface Sci. 438 (2015) 323–331.
[47] W.M. Draper, D.G. Crosby, Photochemistry and volatility of drepamon in water, J. Agric. Food Chem. 32 (1984) 728–733.
[48] J. Lee, W. Choi, Effect of platinum deposits on TiO_2 on the anoxic photocatalytic degradation pathways of alkylamines in water: dealkylation and N-alkylation, Environ. Sci. Technol. 38 (2004) 4026–4033.
[49] M.A. Fox, A.A. Abdel-Wahad, Selectivity in the TiO_2-mediated photocatalytic oxidation of thioethers, Tetrahedron Lett. 31 (1990) 4533–4536.
[50] E. Evgenidou, I. Konstantinou, K. Fytianos, T. Albanis, Study of the removal of dichlorvos and dimethoate in a titanium dioxide mediated photocatalytic process through the examination of intermediates and the reaction mechanism, J. Hazard. Mater. B 137 (2006) 1056–1064.
[51] M. Kerzhentsev, C. Guillard, J.-M. Herrmann, P. Pichat, Photocatalytic pollutant removal in water at room temperature: case study of the total degradation of the insecticide fenitrothion (phosphorothioic acid O, O-dimethyl-O-(3-methyl-4-nitrophenyl) ester), Catal. Today 27 (1996) 215–220.